The SunCHECK™ Platform powers Quality Management in radiation therapy.

Scalable to meet the needs of any clinic or network, SunCHECK helps:

- **Reduce risks**
- **Control costs**
- **Improve treatment quality**

Visit sunnuclear.com to learn how SunCHECK fits into your clinic.

Patient Safety Starts Here

SUN NUCLEAR corporation

Received: 9 September 2021 | Revised: 11 January 2022 | Accepted: 12 January 2022

DOI: 10.1002/mp.15473

RESEARCH ARTICLE

MEDICAL PHYSICS

Design, realization, and characterization of a novel diamond detector prototype for FLASH radiotherapy dosimetry

Marco Marinelli[1] | **Giuseppe Felici**[2] | **Federica Galante**[2] | **Alessia Gasparini**[3,4] | **Lucia Giuliano**[5] | **Sophie Heinrich**[5] | **Matteo Pacitti**[2] | **Giuseppe Prestopino**[1] | **Verdi Vanreusel**[3,4] | **Dirk Verellen**[3,4] | **Claudio Verona**[1] | **Gianluca Verona Rinati**[1]

[1] Industrial Engineering Department, University of Rome "Tor Vergata", Rome, Italy

[2] SIT S.p.A., Aprilia, Latina, Italy

[3] Iridium Kankernetwerk, Antwerp, Belgium

[4] University of Antwerp, Antwerp, Belgium

[5] Institut Curie, Inserm U 1021-CNRS UMR 3347, University Paris-SaclayPSL Research University, Orsay, France

Correspondence
Gianluca Verona Rinati, Department Industrial Engineering, University of Rome "Tor Vergata", Via del Politecnico 1, 00133 Roma, Italy.
Email: gianluca.verona.rinati@uniroma2.it

Funding information
European Metrology Programme for Innovation and Research; European Union's Horizon 2020 Research and Innovation

Abstract

Purpose: FLASH radiotherapy (RT) is an emerging technique in which beams with ultra-high dose rates (UH-DR) and dose per pulse (UH-DPP) are used. Commercially available active real-time dosimeters have been shown to be unsuitable in such conditions, due to severe response nonlinearities. In the present study, a novel diamond-based Schottky diode detector was specifically designed and realized to match the stringent requirements of FLASH-RT.

Methods: A systematic investigation of the main features affecting the diamond response in UH-DPP conditions was carried out. Several diamond Schottky diode detector prototypes with different layouts were produced at Rome Tor Vergata University in cooperation with PTW-Freiburg. Such devices were tested under electron UH-DPP beams. The linearity of the prototypes was investigated up to DPPs of about 26 Gy/pulse and dose rates of approximately 1 kGy/s. In addition, percentage depth dose (PDD) measurements were performed in different irradiation conditions. Radiochromic films were used for reference dosimetry.

Results: The response linearity of the diamond prototypes was shown to be strongly affected by the size of their active volume as well as by their series resistance. By properly tuning the design layout, the detector response was found to be linear up to at least 20 Gy/pulse, well into the UH-DPP range conditions. PDD measurements were performed by three different linac applicators, characterized by DPP values at the point of maximum dose of 3.5, 17.2, and 20.6 Gy/pulse, respectively. The very good superimposition of three curves confirmed the diamond response linearity. It is worth mentioning that UH-DPP irradiation conditions may lead to instantaneous detector currents as high as several mA, thus possibly exceeding the electrometer specifications. This issue was properly addressed in the case of the PTW UNIDOS electrometers.

Conclusions: The results of the present study clearly demonstrate the feasibility of a diamond detector for FLASH-RT applications.

KEYWORDS
diamond detector, dosimetry, FLASH radiotherapy

1 | INTRODUCTION

FLASH radiation therapy is being extensively studied by many research groups and institutions as a promising technique to treat tumors. It has been reported that an irradiation modality making use of ultra-high dose rates (UH-DR) greater than 40 Gy/s[1,2] results in improved sparing of healthy tissues while preserving its effectiveness in treating cancerous cells.[3–14] In addition, recent preclinical studies increasingly support the clinical translation of FLASH radiotherapy (RT).[15–18] In most studies on the FLASH effect, dedicated electron accelerators[19–23] or modified clinical linear accelerators[24–26] were used, delivering electron pulses of ultra-high dose per pulse (UH-DPP) in the range from 0.5 to 10 Gy/pulse. However, these somewhat extreme irradiation conditions are indeed challenging in terms of dosimetry.[11,20,22,26–30] As a matter of fact, only passive dosimetric systems (basically alanine,[31,32] Gafchromic films,[33] and thermo-luminescent dosimeters[28]) have been successfully used at present, provided that specific irradiation protocols are adopted. A delay of hours or even days can be needed in order to get the response from the passive detector irradiation. Besides, the accuracy in the dose determination by any of the above mentioned detectors is no better than a few percent.

Due to such drawbacks of passive dosimetry, active real-time dosimetric systems would be highly preferred. However, all the commercially available active dosimeters have been shown to suffer from serious issues at UH-DPP values, such as dose rate dependence, saturation effect, and strong nonlinearity of their response.[22,28,29,34]

Ionization chambers (ICs) are well assessed reference dosimeters in conventional radiation therapy techniques. However, a noticeable decrease in their ion collection efficiency has been observed when the DPP value exceeds 0.1 Gy/pulse,[34–38] due to direct recombination and polarization effects. Recently, the suitability of a transportable aluminum calorimeter as real-time detector for the accurate dosimetry of electron beams with UH-DPP has been demonstrated.[27,32] However, the use of this dosimetric system in clinical environments is often impractical. As far as solid-state detectors are concerned, silicon diodes exhibit response nonlinearities as a function of the DPP.[25,39] In addition, the effect of radiation damage is to be considered as well, further limiting the suitability of such detectors in FLASH-RT.[11] The PTW 60019 diamond detector, developed by some of the authors at Rome Tor Vergata University in cooperation with PTW-Freiburg, is well assessed in conventional RT dosimetry, due to its near tissue equivalence, radiation hardness, and good spatial resolution.[40–45] Nevertheless, Di Martino et al.[22] reported a signal nonlinearity from such detector at DPP values greater than about 0.1 Gy/pulse as well. From all of the above, there's a need for a reliable solid-state active dosimeter capable of taking on the challenging irradiation conditions typically used in FLASH-RT.

In the present study, a systematic investigation of the main physical properties affecting the diamond response in UH-DPP conditions was carried out, aimed at developing a novel diamond detector, namely a FLASH diamond (fD), specifically designed for FLASH-RT applications. A comprehensive dosimetric and metrological characterization of such a detector is currently ongoing, by the partners of the UHDpulse European project.

2 | MATERIALS AND METHODS

The PTW 60019 microDiamond (mD) is basically a Schottky diode, characterized by a sensitivity of approximately 1 nC/Gy.[44–46] Its active volume consists of an intrinsic diamond layer deposited on top of a conductive p-type boron-doped diamond layer, which is used as a back contact. The electrical connection of the device to the triaxial cable is obtained by a metallic Schottky contact onto the intrinsic layer and an ohmic metallic contact on the boron-doped diamond layer. Such a device is operating at zero external bias voltage. An internal electric field is produced by the built-in potential of about 1 V due to the Schottky contact, allowing for the collection of the electron hole pairs generated by the impinging radiation. Now, if we assume a typical UH-DPP irradiation condition with a DPP of 1 Gy/pulse in 1 μs, this would lead to an instantaneous dose rate (i.e., the dose rate during the pulse duration) of 1 MGy/s and an instantaneous current of 1 mA. This implies that a series resistance of 1 kΩ would produce a 1 V voltage drop opposite to the internal built-in potential, inhibiting the detector operation. A saturation of the device response is then expected, the higher the series resistance the lower the DPP value up to which the detector shows a linear response. It is worth noticing that, when considering a diode detector, series resistances even much higher than 1 kΩ are easily reached.[47,48] This can be ascribed to: (1) the Schottky contact resistance; (2) the drift resistance in the depletion region of the intrinsic diamond; (3) the electrical resistance of the boron-doped layer; (4) the contact resistance at the metal to boron-doped layer interface. Therefore, in principle, the range of linear operation of the diode detector can be extended to higher DPPs either by limiting the detection current through a reduction of the detector sensitivity and/or by decreasing the series resistance of the detector.

In the present study, a systematic investigation was performed in order to tune the layout and properties of the mD detector in view of FLASH therapy applications. Several diamond prototypes were produced by properly modifying their design and production processes. More

TABLE 1 List of the diamond detector prototypes investigated in the present study

Sample ID	Active area (mm^2)	Boron concentration	Sensitivity (nC/Gy)
DD-1.0	0.79	Standard	0.228
DD-1.3	1.3	Standard	0.364
DD-1.6	2.0	Standard	0.648
DD-1.9	2.8	Standard	0.828
DD-2.2 (mD)	3.8	Standard	1.120
DD-2.5	4.9	Standard	1.610
DD-P^{+}	3.8	Medium	0.830
DD-P^{++}	3.8	High	1.110
fD-A	1.5	High	0.400
fD-B	1.5	High	0.283

specifically, both the size of the active volume and the boron concentration in the diamond-doped layer were systematically varied. Modifying the former parameter would result in a change of the detector sensitivity, while the latter is expected to affect the contribution to the series resistance described above in points (3) and (4). A summary of the investigated samples is reported in Table 1.

All the detectors were encapsulated in the same housing used by PTW for the standard mD dosimeter. Among the geometrical parameters, it is worth mentioning that the point of measurement is located at a 1 mm water equivalent depth below the top detector surface.

The characterization of the diamond prototypes under UH-DPP irradiation conditions was performed by using electron beams delivered by ElectronFlash linacs (SIT S.p.A., Aprilia, Italy) in two different facilities: SIT S.p.A. and Curie Institute (Orsay, France). The beams produced by such linacs are characterized by electron pulses, whose duration can be varied from 0.5 up to 4 μs, and a maximum pulse repetition frequency (PRF) of 245 Hz. In typical irradiation conditions, DPPs on the order of 10 Gy/s can be reached, thus leading to instantaneous dose rates on the order of several MGy/s and average dose rates on the order of 1 kGy/s. Since the collection time of the diamond diodes is typically much lower than 1 μs, the instantaneous dose rate, and thus the instantaneous current flowing in the detector, are expected to be the most critical parameters to be addressed in order to improve the detector performance in UH-DPP conditions. Nonetheless, the dependence of the detector response on the electron beam PRF is to be carefully investigated as well.

The linac configuration and irradiation parameters adopted at SIT were as follows: beam energy 9 MeV, PRF 5 Hz, pulse duration 4 μs, Polymethyl Methacrylate (PMMA) applicators 100 and 40 mm in diameter, and source to surface distance (SSD) ranging from 73 up to 217 cm. In particular, a DPP range from 0.46 up to 3.93 Gy/pulse was achieved by using the 100 mm applicator, while a 3.83–10.40 Gy/pulse range was obtained by using the 40 mm applicator. The PRF dependence of the detector response was investigated at SIT under 9 MeV irradiations, at the depth of maximum dose deposition d_{max}, with the 100 mm applicator and by varying the PRF from 5 to 245 Hz. A semiflex IC (PTW type 31010, PTW-Freiburg, Germany) was used as a reference, to take into account any variation of the linac output in different PRF conditions. The IC was positioned outside the beam region, 5 cm away from the outer wall of the applicator, so as to avoid response saturation.

Slightly different parameters were used during the tests performed at the Curie Institute: 7 MeV, 10 Hz, 4 μs, seven PMMA applicators (120, 100, 50, 40, 35, 30, and 10 mm in diameter), SSDs from 60 to 171 cm. In such irradiation conditions, the DDP was found to vary from 3.30 up to 26.40 Gy/pulse.

EBT-XD films (Ashland Inc., Bridgewater, NJ, USA) were used for reference dosimetry in both facilities.[11] They were calibrated and analyzed by the FilmQA™ Pro software (Ashland Inc.), according to the protocol suggested by the manufacturer. Calibration was performed in a 7 MeV beam in conventional dose rate mode (5 cGy/pulse, PRF 5 Hz) with the 100 mm applicator. Eight different films were irradiated in a RW3 solid phantom with doses ranging from 0.25 up to 32.0 Gy in geometric progression ($0.25 \times 2n$ Gy, $n = 0, \ldots, 8$), while one was left not irradiated. For each calibration point, dose was measured by means of a PTW Advanced Markus ionization chamber (type 34045, PTW-Freiburg, Germany). Gafchromic film readings were performed both immediately after irradiation (as per the protocol) and 48 h after the irradiation, by using an Epson Expression 12000XL (Epson, USA). Maximum variations between the early and late readings were below 2%.

EBT-XD films were used to evaluate the 2D beam dose distribution as well. Typical dose distribution images are reported in Figure 1 for the case of the 100 and 40 mm applicators during 9 MeV UH-DR irradiations at SIT. A field flatness and symmetry of less than 3% was derived in both cases. A black dot is also added in the center of both field images, indicating the size of the sensitive area of the fD-A and fD-B diamond detector prototypes.

The irradiations for testing the detector response linearity were performed by positioning the diamond prototypes in a cylindrical PMMA phantom, 120 mm in diameter (see Figure 2). As for the percentage depth dose (PDD) measurements, PMMA slabs with increasing thicknesses were positioned in front of the PMMA phantom in order to reach an equivalent depth in water of about 50 mm.

A PTW UNIDOS E electrometer (PTW-Freiburg, Germany) was used at SIT for the acquisition of the diamond signal, while a UNIDOS webline was used at the

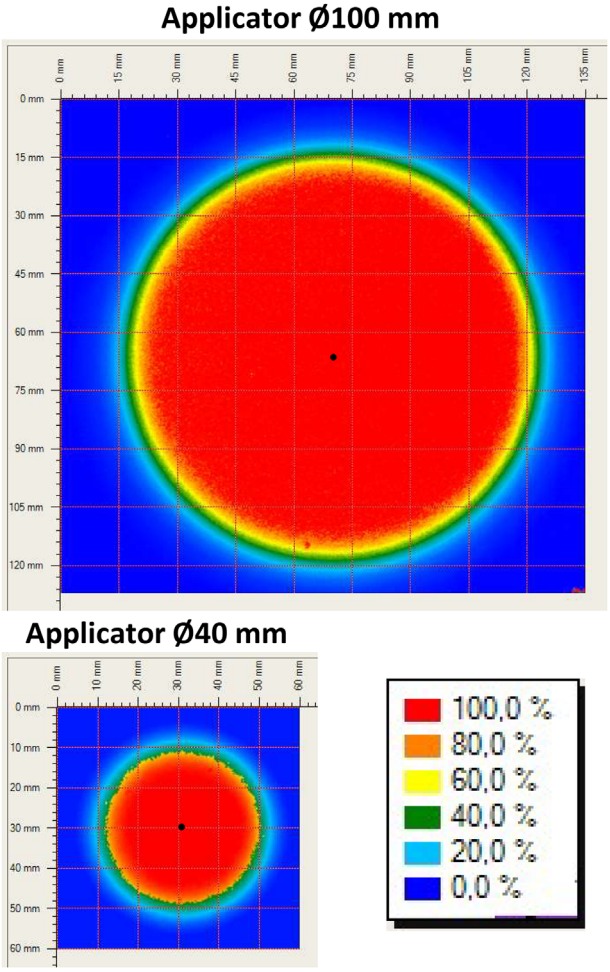

FIGURE 1 Dose distribution images acquired at SIT for the 100 and 40 mm applicators during 9 MeV ultra-high dose rate (UH-DR) irradiations. Black dots in the center of the field images represent the size of the active area of the fD-A and fD-B diamond detector prototypes

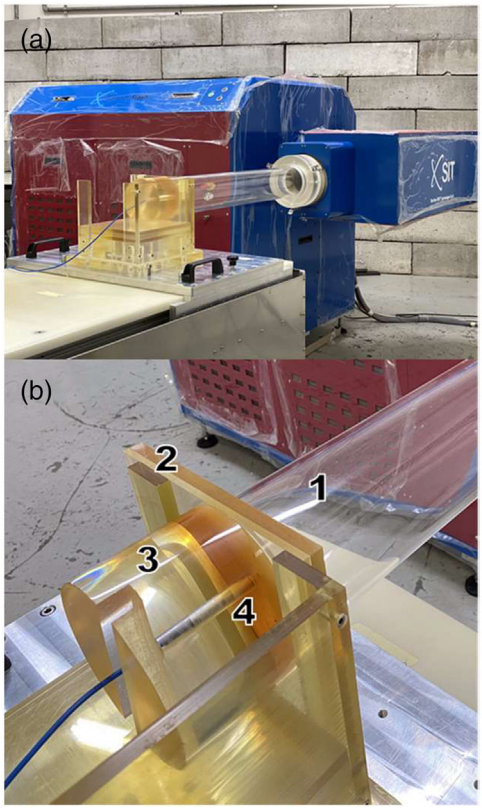

FIGURE 2 (a) Typical irradiation setup used both at SIT and at the Curie Institute. (b) Enlarged view showing in more detail: (1) the linac applicator, (2) the PMMA slabs, (3) the PMMA cylindrical phantom, and (4) the diamond prototype

Curie Institute. It is important to mention that the previously estimated instantaneous current on the order of 1 mA expected in the above described experimental setups is well beyond the measuring range reported in the specifications of the two electrometers. In order to prevent such an issue, an external box was provided by PTW to be connected in between the diamond detector triaxial cable plug and the electrometer signal input. Basically a 100 nF capacitance was used, connected in parallel to the electrometer input, so as to broaden the current pulses from the diamond prototype and avoid too high peak currents at the electrometer input. This technique was proved not to produce artifacts in the test results, by performing measurements by the UNIDOS electrometers with and without the external box, and by comparing the obtained results with the ones recorded in the very same setup and irradiation conditions by using a Keithley 6517B (Keithley Instruments, LLC, Cleveland, OH, USA) electrometer instead. Such a comparison will be shown in Section 3 of the present paper.

3 | RESULTS AND DISCUSSION

In order to test the effect of the detector sensitivity on the performance in UH-DPP irradiation conditions, six prototypes were fabricated, nominally identical to a mD dosimeter, with the only exception being a systematic variation of the active area diameter, from 1.0 up to 2.5 mm. The detector with a 2.2 mm diameter is thus a standard mD detector. The sensitivity of the prototypes was evaluated at the PTW calibration laboratory, under ^{60}Co source irradiation. In Figure 3, the obtained sensitivities are reported as a function of the active area. A linear trend is confirmed by the experimental data and an overall change by a factor of 7 was achieved, with sensitivities ranging from 0.228 to 1.610 nC/Gy. The data scattering in Figure 3 is to be attributed to unintentional relatively small differences in the active layer thickness of the detector prototypes, affecting their sensitivities.

Such detectors were then irradiated at SIT by ElectronFlash linac beams. The following irradiation setup was used: 9 MeV, 100 mm applicator, 15 mm PMMA

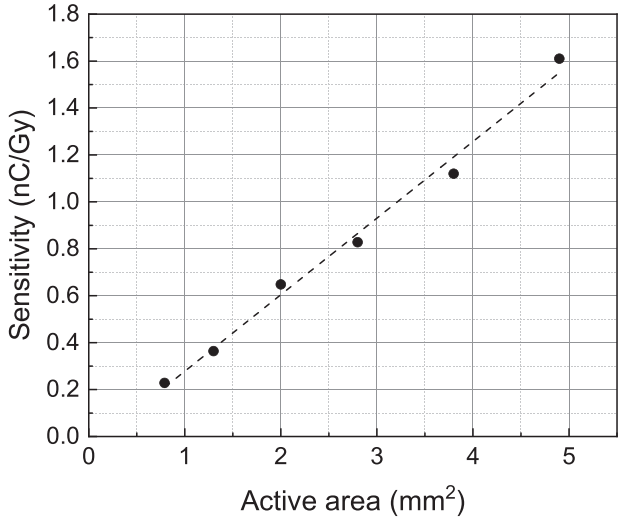

FIGURE 3 Sensitivity of the detectors listed in Table 1 with active area diameter ranging from 1.0 to 2.5 mm (from DD-1.0 to DD-2.5). The dashed line is the linear best fit

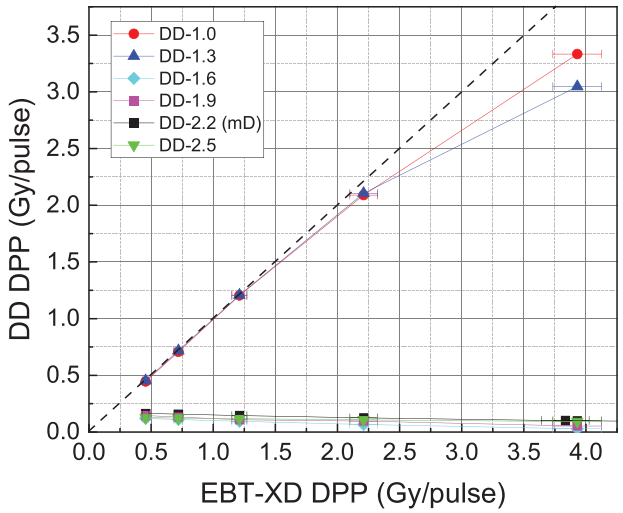

FIGURE 4 Dose per pulse (DPPs) measured by the diamond prototypes with different active area as a function of the DPPs measured by EBT-XD films. The dashed line with slope 1 is reported to evaluate the deviation from linearity of the detector response

build-up to reach d_{max}, SSDs from 106 cm (close contact with the applicator) up to 217 cm, corresponding to a DPP ranging from 0.46 to 3.93 Gy/pulse, as evaluated by EBT-XD Gafchromic films. In Figure 4, the response of the diamond prototypes divided by their sensitivities, that is, the DPP values measured by the diamond detectors, are reported as a function of the EBT-XD DPPs. An error bar of ±5% was adopted for the EBT-XD DPP determination. Such a value was estimated by repeatability tests, and includes both the intrinsic uncertainty of the EBT-XD readings and eventual fluctuations of the accelerator output.

It is clearly observed that all of the prototypes having an active area diameter equal to or larger than 1.6 mm

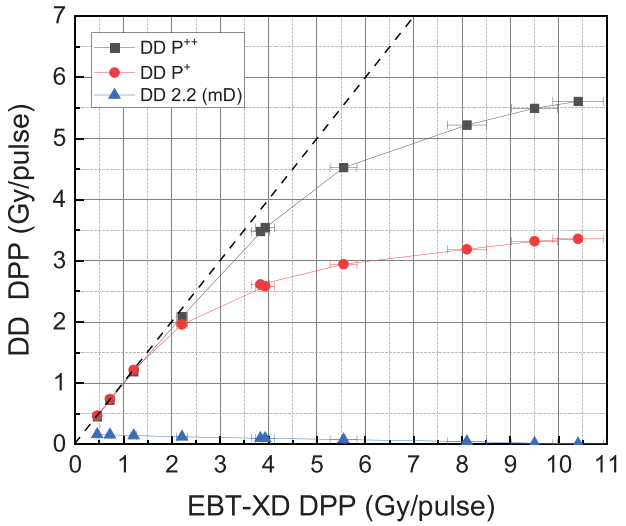

FIGURE 5 Dose per pulse (DPPs) measured by the diamond prototypes with different boron concentration in the diamond-doped layer as a function of the DPPs measured by EBT-XD films. The dashed line with slope 1 is reported to evaluate the deviation from linearity of the detector response

exhibit a completely saturated response, even at the smallest DPP of 0.46 Gy/pulse. This behavior is consistent with that reported by Di Martino et al.[22] for the "standard" mD. On the contrary, a linear response at least up to about 1.2 Gy/pulse is obtained by the prototypes with smaller active areas. In particular, a more pronounced deviation from linearity is observed at 3.9 Gy/pulse for DD-1.3 with respect to DD-1.0, thus confirming the hypothesis that the smaller the sensitivity the better in terms of response linearity.

The effect of a change in the series resistance of the diamond detector was then investigated. To this purpose, a set of three prototypes was used, all of them nominally identical to the standard mD, the only difference being the boron concentration of the p-type layer. More specifically, sample DD-2.2 is indeed a standard mD, while the samples DD-P^+ and DD-P^{++} were produced with an increased boron concentration in the p-type layer, resulting in a decrease of their resistivity by one order and two orders of magnitude, respectively, as compared to the one of sample DD-2.2. The responses of the three detectors are reported in Figure 5.

The obtained results confirm the hypothesis that reducing the overall detector series resistance results in an improved linearity range. In particular, the response of both the prototypes with higher boron concentration in the p-type layer start saturating at about 1.2 Gy/pulse, the deviation from linearity at higher DPPs being definitively more pronounced in the DD-P^+ sample.

A specific detector layout was then chosen in order to combine the positive effects observed in both the above reported systematic investigations. In particular, two fD prototypes were fabricated (fD-A and fD-B), both with a

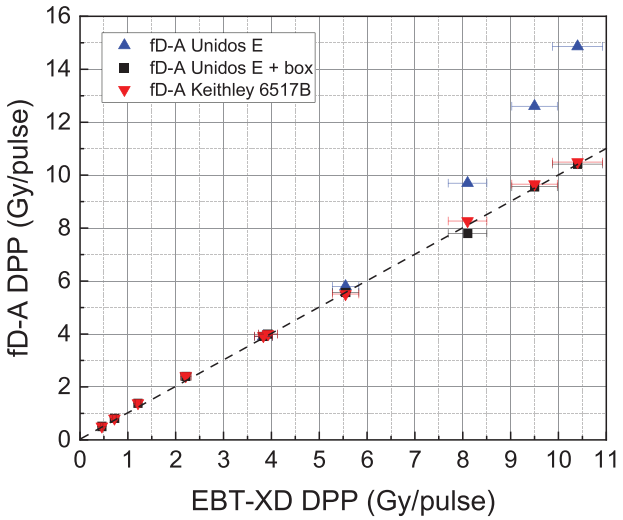

FIGURE 6 Dose per pulse (DPPs) measured by the fD-A prototype at SIT. The three datasets refer to the measurements performed by: the UNIDOS E electrometer alone (blue triangles), the UNIDOS E equipped with the external capacitance box (black squares), and the Keithley 6517B electrometer (red triangles). The dashed line with slope 1 is reported to evaluate the deviation from linearity of the detector response

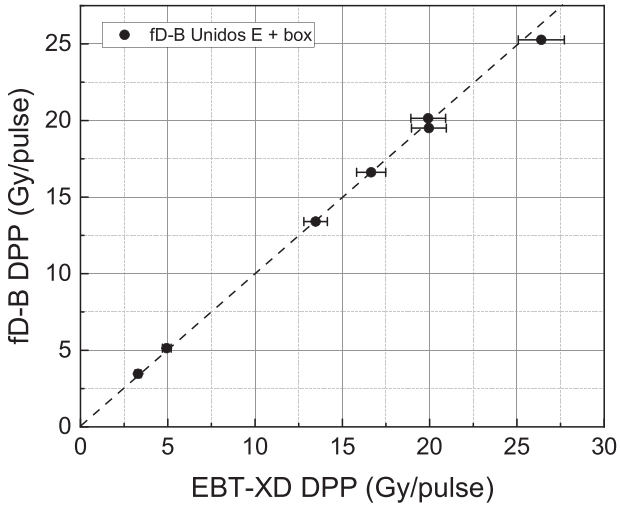

FIGURE 7 Dose per pulse (DPPs) measured by the fD-B prototype at the Curie Institute. The dashed line with slope 1 is reported to evaluate the deviation from linearity of the detector response

1.4 mm active area diameter and a P^{++} boron-doped layer. Such detectors were independently characterized under ElectronFlash linac irradiation conditions in two different facilities: fD-A at SIT and fD-B at the Curie Institute.

The SIT test results on the fD-A prototype are reported in Figure 6. Three different electronic readout setups were used in order to verify the presence of any artifact ascribed to an eventual incorrect operation of the adopted electrometer. They were acquired by using: the UNIDOS E electrometer alone (blue triangles), the UNIDOS E equipped with the external capacitance box (black squares), and the Keithley 6517B electrometer (red triangles). Indeed, a super-linearity is clearly observed in the case in which the UNIDOS E alone was used, which is to be ascribed to the electrometer being operated well beyond its specifications, that is for measuring peak detector currents exceeding the threshold value indicated by the electrometer manufacturer. It's worth noting that such an effect was not observed in the previous plots due to the "early" saturation of the prototype response. This issue was overcome by adopting the external capacitance box provided by PTW. In fact, the experimental data obtained by the UNIDOS E in this modified setup (UNIDOS E + box in Figure 6) are found to be fully consistent with those obtained by the Keithley 6517B electrometer.

As far as the response of the fD-A detector is concerned, it is found to be linear up to a DPP of 10.4 Gy/pulse, that is the maximum value achievable by using the 40 mm applicator. This finding clearly confirms the physical hypothesis of the present systematic investigation as well as the effectiveness of the changes made in the diamond detector design and layout.

The fD-B detector was characterized at the Curie Institute. A response linearity test was first performed by using all the available applicators listed in Section 2. In all cases an 11 mm PMMA slab was used to reach d_{max}, with the only exception being the 10 mm applicator in which case a 5 mm slab was used instead to take account of the shift of d_{max} towards the surface for small fields. In each case, the measurement was performed by positioning the diamond detector with the build-up slab in close contact with the applicator. In addition, an EBT-XD Gafchromic film was sandwiched in between the build-up slab and the fD-B top surface for simultaneous irradiation of both dosimetric systems. The results of this test are reported in Figure 7, where an error bar of ±5% was again adopted for the EBT-XD DPP determination.

The device response was found to be linear up to about 26 Gy/pulse, within the experimental uncertainty. However, it should be pointed out that, due to the UH-DPPs delivered when using the applicators with a diameter equal to or less than 50 mm, only one single pulse could be delivered in order to avoid any saturation of the EBT-XD film response. Better statistics would be needed in order to improve the measurement accuracy.

PDD measurements were then performed by the fD-B prototype, by using PMMA slabs with increasing thicknesses. Three different applicators were used for this purpose, namely the 120, 40, and 30 mm, in which cases a DPP values of 3.5, 17.2, and 20.6 Gy/pulse were obtained respectively at d_{max}. In these conditions, nearly identical PDD curves would be expected given that the beam size is larger, or similar in the 30 mm case, than the lateral equilibrium range.[49] So, among other things,

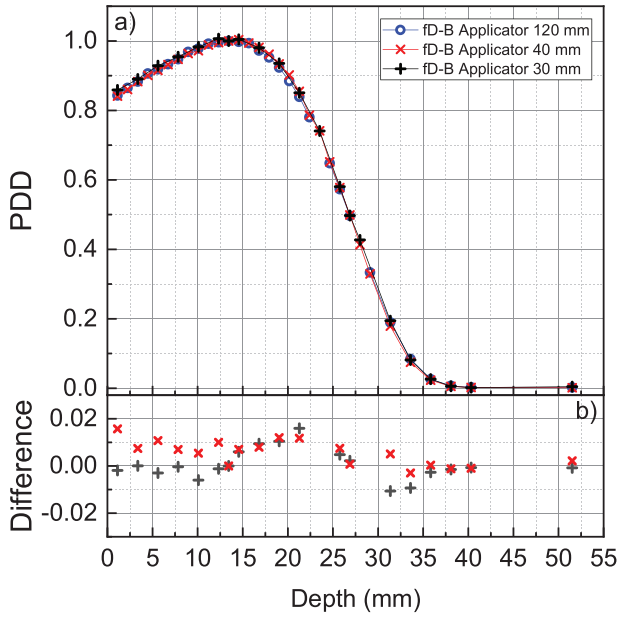

FIGURE 8 (a) Percentage depth dose (PDD) measurements by the fD-B prototype at Curie Institute. The three datasets refer to the measurements performed by using the 120, 40, and 30 mm applicators, characterized by a dose per pulse (DPP) values at d_{max} of 3.5, 17.2, and 20.6 Gy/pulse, respectively. (b) Difference plot between the PDDs measured by using the 40 and 30 mm applicators and the one measured by the 120 mm applicator (black and red symbols, respectively)

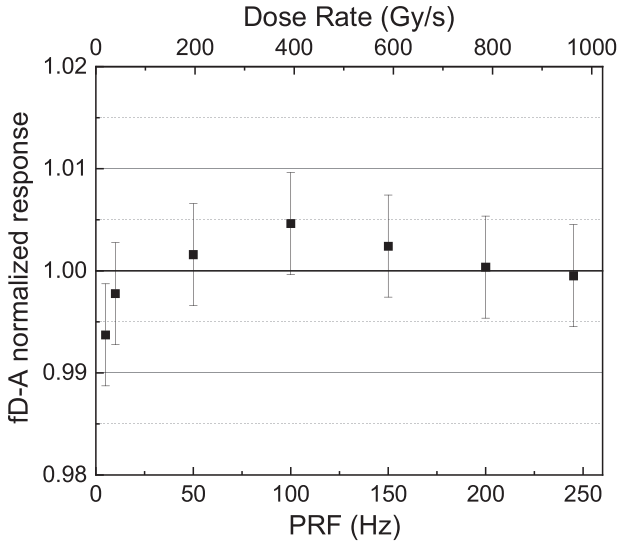

FIGURE 9 Normalized ratio between the fD-A detector and the reference ionization chamber (IC) responses as a function of the pulse repetition frequency (PRF) (lower *x* axis) and the average dose rate (DR) (upper *x*-axis)

this test allows for an independent verification of the response linearity of the fD-B prototype. The obtained results are reported in Figure 8 as a function of the equivalent depth in water.

The three measured PDD curves nicely superimpose one with each other (see Figure 8a). This is more quantitatively shown in Figure 8b, in which the difference plot between the PDDs measured by using the 40 and 30 mm applicators and the one from the 120 mm applicator is reported. The fluctuation of about 3% observed in Figure 8b is compatible with the statistical scattering of the data typically observed in the experimental conditions adopted in the present work. The results reported in Figure 8 also imply that the response of the fD-B prototype is independently confirmed to be linear at least up to a DPP of 20.6 Gy/pulse.

The fD-A prototype response was finally investigated as a function of the beam PRF. In particular, the PRF was varied from 5 up to 245 Hz, corresponding to an average DR changing from about 2 to 960 Gy/s, the average DR being equal to the product of DPP and PRF. The normalized ratio between the readings of fD-A and the semiflex IC is reported in Figure 9, in which variations of about ±0.5% may be noticed, comparable with experimental uncertainty. This implies than a very small dependency of the detector response, if any, is demonstrated up a DR of about 1 kGy/s.

4 | CONCLUSIONS

A systematic investigation was performed on the properties of diamond-based detectors aimed at designing, realizing and characterizing a novel dosimeter for FLASH therapy applications. The study was based on the assumption that a fine tuning of the physical properties of the produced prototypes would allow them to meet the challenging requirements of FLASH-RT dosimetry. Several diamond detectors were thus realized by systematically varying their active area (and thus sensitivity) as well as boron concentration in the p-type layer (and thus series resistance). They were tested under ElectronFlash linac irradiation in different setup conditions, by using EBT-XD Gafchromic films as reference dosimeters. Based on the obtained results, two fD prototypes were finally realized and independently characterized in two different facilities. Their response linearity was evaluated as a function of the DPP up to a maximum of 26 Gy/pulse. PDDs were measured in three different setup conditions, characterized by DPP values at d_{max} of 3.5, 17.2, and 20.6 Gy/pulse, respectively. The obtained experimental results confirm a response linearity of fD prototypes up to at least 20 Gy/pulse, well in the UH-DPP range. In addition, the effect of an electron beam PRF variation in the range from 5 up to 245 Hz, corresponding to DRs from about 2 to 960 Gy/s, was also investigated. The detector response was found to independent from the PRF within ±0.5%. This clearly demonstrates the feasibility of a diamond detector for FLASH-RT applications. Work is in progress to perform a comprehensive dosimetric characterization of the proposed fD detectors.

ACKNOWLEDGMENTS

The present work is part of the 18HLT04 UHDpulse project (http://uhdpulse-empir.eu/) which has received funding from the European Metrology Programme for Innovation and Research (EMPIR) program, co-financed by the Participating States and from the European Union's Horizon 2020 Research and Innovation program. We wish to thank PTW-Freiburg for cooperation in the diamond prototype production. We also thank Rafael Kranzer (PTW-Freiburg) and Andreas Schüller (Physikalisch-Technische Bundesanstalt, PTB) for helpful discussions.

CONFLICT OF INTERESTS

Marco Marinelli and Gianluca Verona Rinati, signed a contract with PTW-Freiburg involving financial interests deriving from the PTW microDiamond 60019 dosimeter commercialization. Giuseppe Felici is SIT S.p.A. shareholder. Matteo Pacitti and Federica Galante are employees at SIT S.p.A. Alessia Gasparini received a grant for a post doc position funded by SIT S.p.A.

REFERENCES

1. Favaudon V, Caplier L, Monceau V, et al. Ultrahigh dose-rate FLASH irradiation increases the differential response between normal and tumor tissue in mice. *Sci Transl Med*. 2014;6(245):245ra93. https://doi.org/10.1126/scitranslmed.3008973
2. Fouillade C, Favaudon V, Vozenin M-C, et al. Les promesses du haut débit de dose en radiothérapie. *Bull Cancer*. 2017;104(4):380-384. https://doi.org/10.1016/j.bulcan.2017.01.012
3. Montay-Gruel P, Petersson K, Jaccard M, et al. Irradiation in a flash: unique sparing of memory in mice after whole brain irradiation with dose rates above 100 Gy/s. *Radiother Oncol*. 2017;124(3):365-369. https://doi.org/10.1016/j.radonc.2017.05.003
4. Durante M, Brauer-Krisch E, Hill M. Faster and safer? FLASH ultra-high dose rate in radiotherapy. *Br J Radiol*. 2018;91(1082):20170628. https://doi.org/10.1259/bjr.20170628
5. Patriarca A, Fouillade C, Auger M, et al. Experimental set-up for FLASH proton irradiation of small animals using a clinical system. *Int J Radiat Oncol Biol Phys*. 2018;102(3):619-626. https://doi.org/10.1016/j.ijrobp.2018.06.403
6. Montay-Gruel P, Bouchet A, Jaccard M, et al. X-rays can trigger the FLASH effect: ultra-high dose-rate synchrotron light source prevents normal brain injury after whole brain irradiation in mice. *Radiother Oncol*. 2018;129(3):582-588. https://doi.org/10.1016/j.radonc.2018.08.016
7. Montay-Gruel P, Acharya MM, Petersson K, et al. Long-term neurocognitive benefits of FLASH radiotherapy driven by reduced reactive oxygen species. *Proc Natl Acad Sci USA*. 2019;116(22):10943-10951. https://doi.org/10.1073/pnas.1901777116
8. Vozenin M-C, De Fornel P, Petersson K, et al. The advantage of FLASH radiotherapy confirmed in mini-pig and cat-cancer patients. *Clin Cancer Res*. 2019;25(1):35-42. https://doi.org/10.1158/1078-0432.CCR-17-3375
9. Vozenin M-C, Hendry JH, Limoli CL. Biological benefits of ultra-high dose rate FLASH radiotherapy: sleeping beauty awoken. *Clin Oncol*. 2019;31(7):407-415. https://doi.org/10.1016/j.clon.2019.04.001
10. Simmons DA, Lartey FM, Schüler E, et al. Reduced cognitive deficits after FLASH irradiation of whole mouse brain are associated with less hippocampal dendritic spine loss and neuroinflammation. *Radiother Oncol*. 2019;139:4-10. https://doi.org/10.1016/j.radonc.2019.06.006
11. Esplen N, Mendonca MS, Bazalova-Carter M. Physics and biology of ultrahigh dose-rate (FLASH) radiotherapy: a topical review. *Phys Med Biol*. 2020;65(23):23TR03. https://doi.org/10.1088/1361-6560/abaa28
12. Hughes JR, Parsons JL. FLASH radiotherapy: current knowledge and future insights using proton-beam therapy. *IJMS*. 2020;21(18):6492. https://doi.org/10.3390/ijms21186492
13. Wilson JD, Hammond EM, Higgins GS, Petersson K. Ultra-high dose rate (FLASH) radiotherapy: silver bullet or fool's gold? *Front Oncol*. 2020;9:1563. https://doi.org/10.3389/fonc.2019.01563
14. Lin B, Gao F, Yang Y, et al. FLASH radiotherapy: history and future. *Front Oncol*. 2021;11:644400. https://doi.org/10.3389/fonc.2021.644400
15. Bourhis J, Montay-Gruel P, Gonçalves Jorge P, et al. Clinical translation of FLASH radiotherapy: why and how? *Radiother Oncol*. 2019;139:11-17. https://doi.org/10.1016/j.radonc.2019.04.008
16. Bourhis J, Sozzi WJ, Jorge PG, et al. Treatment of a first patient with FLASH-radiotherapy. *Radiother Oncol*. 2019;139:18-22. https://doi.org/10.1016/j.radonc.2019.06.019
17. Buonanno M, Grilj V, Brenner DJ. Biological effects in normal cells exposed to FLASH dose rate protons. *Radiother Oncol*. 2019;139:51-55. https://doi.org/10.1016/j.radonc.2019.02.009
18. Vozenin M-C, Baumann M, Coppes RP, Bourhis J. FLASH radiotherapy international workshop. *Radiother Oncol*. 2019;139:1-3. https://doi.org/10.1016/j.radonc.2019.07.020
19. Jaccard M, Durán MT, Petersson K, et al. High dose-per-pulse electron beam dosimetry: commissioning of the Oriatron eRT6 prototype linear accelerator for preclinical use. *Med Phys*. 2018;45(2):863-874. https://doi.org/10.1002/mp.12713
20. Jorge PG, Jaccard M, Petersson K, et al. Dosimetric and preparation procedures for irradiating biological models with pulsed electron beam at ultra-high dose-rate. *Radiother Oncol*. 2019;139:34-39. https://doi.org/10.1016/j.radonc.2019.05.004
21. Lansonneur P, Favaudon V, Heinrich S, Fouillade C, Verrelle P, De Marzi L. Simulation and experimental validation of a prototype electron beam linear accelerator for preclinical studies. *Phys Med*. 2019;60:50-57. https://doi.org/10.1016/j.ejmp.2019.03.016
22. Di Martino F, Barca P, Barone S, et al. FLASH radiotherapy with electrons: issues related to the production, monitoring, and dosimetric characterization of the beam. *Front Phys*. 2020;8:570697. https://doi.org/10.3389/fphy.2020.570697
23. Faillace L, Barone S, Battistoni G, et al. Compact S-band linear accelerator system for ultrafast, ultrahigh dose-rate radiotherapy. *Phys Rev Accel Beams*. 2021;24(5):050102. https://doi.org/10.1103/PhysRevAccelBeams.24.050102
24. Schueler E, Trovati S, King G, et al. TU-H-CAMPUS-TeP2-02: FLASH irradiation improves the therapeutic index following GI tract irradiation. *Med Phys*. 2016;43(6Part37):3783-3783. https://doi.org/10.1118/1.4957690
25. Lempart M, Blad B, Adrian G, et al. Modifying a clinical linear accelerator for delivery of ultra-high dose rate irradiation. *Radiother Oncol*. 2019;139:40-45. https://doi.org/10.1016/j.radonc.2019.01.031
26. Szpala S, Huang V, Zhao Y, et al. Dosimetry with a clinical linac adapted to FLASH electron beams. *J Appl Clin Med Phys*. 2021;22(6):50-59. https://doi.org/10.1002/acm2.13270
27. Schüller A, Heinrich S, Fouillade C, et al. The European Joint Research Project UHDpulse – metrology for advanced radiotherapy using particle beams with ultra-high pulse dose rates. *Phys Med*. 2020;80:134-150. https://doi.org/10.1016/j.ejmp.2020.09.020

28. Ashraf MR, Rahman M, Zhang R, et al. Dosimetry for FLASH radiotherapy: a review of tools and the role of radioluminescence and Cherenkov emission. *Front Phys*. 2020;8:328. https://doi.org/10.3389/fphy.2020.00328
29. Kim MM, Darafsheh A, Schuemann J, et al. Development of ultra-high dose rate (FLASH) particle therapy. *IEEE Trans Radiat Plasma Med Sci*. 2021:1-1. https://doi.org/10.1109/TRPMS.2021.3091406
30. Kokurewicz K, Schüller A, Brunetti E, et al. Dosimetry for new radiation therapy approaches using high energy electron accelerators. *Front Phys*. 2020;8:568302. https://doi.org/10.3389/fphy.2020.568302
31. Gondré M, Jorge PG, Vozenin M-C, et al. Optimization of alanine measurements for fast and accurate dosimetry in FLASH radiation therapy. *Radiat Res*. 2020;194(6):573-579. https://doi.org/10.1667/RR15568.1
32. Bourgouin A, Schüller A, Hackel T, et al. Calorimeter for real-time dosimetry of pulsed ultra-high dose rate electron beams. *Front Phys*. 2020;8:567340. https://doi.org/10.3389/fphy.2020.567340
33. Jaccard M, Petersson K, Buchillier T, et al. High dose-per-pulse electron beam dosimetry: usability and dose-rate independence of EBT3 Gafchromic films. *Med Phys*. 2017;44(2):725-735. https://doi.org/10.1002/mp.12066
34. Petersson K, Jaccard M, Germond J-F, et al. High dose-per-pulse electron beam dosimetry - a model to correct for the ion recombination in the advanced Markus ionization chamber. *Med Phys*. 2017;44(3):1157-1167. https://doi.org/10.1002/mp.12111
35. Konradsson E, Ceberg C, Lempart M, et al. Correction for ion recombination in a built-in monitor chamber of a clinical linear accelerator at ultra-high dose rates. *Radiat Res*. 2020;194(6):580-586. https://doi.org/10.1667/RADE-19-00012
36. McManus M, Romano F, Lee ND, et al. The challenge of ionisation chamber dosimetry in ultra-short pulsed high dose-rate very high energy electron beams. *Sci Rep*. 2020;10(1):9089. https://doi.org/10.1038/s41598-020-65819-y
37. Poppinga D, Kranzer R, Farabolini W, et al. VHEE beam dosimetry at CERN linear electron accelerator for research under ultra-high dose rate conditions. *Biomed Phys Eng Express*. 2021;7(1):015012. https://doi.org/10.1088/2057-1976/abcae5
38. Kranzer R, Poppinga D, Weidner J, et al. Ion collection efficiency of ionization chambers in ultra-high dose-per-pulse electron beams. *Med Phys*. 2021;48(2):819-830. https://doi.org/10.1002/mp.14620
39. Vignati A, Giordanengo S, Fausti F, et al. Beam monitors for tomorrow: the challenges of electron and photon FLASH RT. *Front Phys*. 2020;8:375. https://doi.org/10.3389/fphy.2020.00375
40. Ciancaglioni I, Marinelli M, Milani E, et al. Dosimetric characterization of a synthetic single crystal diamond detector in clinical radiation therapy small photon beams: dosimetric characterization of a synthetic single crystal diamond detector. *Med Phys*. 2012;39(7Part1):4493-4501. https://doi.org/10.1118/1.4729739
41. Di Venanzio C, Marinelli M, Milani E, et al. Characterization of a synthetic single crystal diamond Schottky diode for radiotherapy electron beam dosimetry: synthetic diamond for radiotherapy electron beam dosimetry. *Med Phys*. 2013;40(2):021712. https://doi.org/10.1118/1.4774360
42. Pillon M, Angelone M, Aielli G, et al. Radiation tolerance of a high quality synthetic single crystal chemical vapor deposition diamond detector irradiated by 14.8 MeV neutrons. *J Appl Phys*. 2008;104:054513. https://doi.org/10.1063/1.2973668
43. Francescon P, Kilby W, Noll JM, Masi L, Satariano N, Russo S. Monte Carlo simulated corrections for beam commissioning measurements with circular and MLC shaped fields on the CyberKnife M6 System: a study including diode, microchamber, point scintillator, and synthetic microdiamond detectors. *Phys Med Biol*. 2017;62(3):1076-1095. https://doi.org/10.1088/1361-6560/aa5610
44. Marinelli M, Prestopino G, Verona C, Verona-Rinati G. Experimental determination of the PTW 60019 microDiamond dosimeter active area and volume: PTW microDiamond active surface area and active volume. *Med Phys*. 2016;43(9):5205-5212. https://doi.org/10.1118/1.4961402
45. De Coste V, Francescon P, Marinelli M, et al. Is the PTW 60019 microDiamond a suitable candidate for small field reference dosimetry? *Phys Med Biol*. 2017;62(17):7036-7055. https://doi.org/10.1088/1361-6560/aa7e59
46. Almaviva S, Marinelli M, Milani E, et al. Chemical vapor deposition diamond based multilayered radiation detector: physical analysis of detection properties. *J Appl Phys*. 2010;107(1):014511. https://doi.org/10.1063/1.3275501
47. Sze SM, Ng KK. *Physics of Semiconductor Devices*. 3rd ed. Wiley-Interscience; 2007.
48. Kübarsepp T, Haapalinna A, Kärhä P, Ikonen E. Nonlinearity measurements of silicon photodetectors. *Appl Opt*. 1998;37(13):2716. https://doi.org/10.1364/AO.37.002716
49. Rosenberg I. Radiation oncology physics: a handbook for teachers and students. *Br J Cancer*. 2008;98:1020. https://doi.org/10.1038/sj.bjc.6604224

How to cite this article: Marinelli M, Felici G, Galante F, et al. Design, realization, and characterization of a novel diamond detector prototype for FLASH radiotherapy dosimetry. *Med. Phys.* 2022;49:1902–1910. https://doi.org/10.1002/mp.15473